Phytochemistry 71 (2010) 1474–1484

Contents lists available at ScienceDirect

Phytochemistry

journal homepage: www.elsevier.com/locate/phytochem

Characterization of a *Vitis vinifera* cv. Cabernet Sauvignon 3′,5′-*O*-methyltransferase showing strong preference for anthocyanins and glycosylated flavonols

Joost Lücker [a,1], Stefan Martens [b], Steven T. Lund [a,*]

[a] Faculty of Land and Food Systems, Wine Research Centre, University of British Columbia, Vancouver, B.C., Canada V6T 1Z4
[b] Fondazione Edmund Mach, Istituto Agrario San Michele all'Adige – IASMA, Centro Ricerca e Innovazione, Area Alimentazione, Via E. Mach 1, 38010 San Michele all'Adige (TN), Italy

ARTICLE INFO

Article history:
Received 16 September 2009
Received in revised form 12 May 2010
Available online 30 June 2010

Keywords:
Vitis vinifera
Vitaceae
Grapevine
Enzyme kinetics
Anthocyanin
Flavonol
O-methyltransferase
Delphinidin 3-*O*-glucoside
Cyanidin 3-*O*-glucoside
Malvidin 3-*O*-glucoside

ABSTRACT

At ripening initiation in red grapevine (*Vitis vinifera*) berries, the exocarp turns color from green to red and then to purple due to the accumulation and extent of methylation of anthocyanins. The accumulation of transcripts encoding an *O*-methyltransferase was recently shown to be closely correlated with the onset of ripening and the degree of blue/purple pigmentation in grapevine berries; however, the biochemical function of this gene has remained uncharacterized. In this study, an *O*-methyltransferase cDNA that showed a distinct expression pattern when compared to closely related sequences was expressed in *Escherichia coli* and enzyme assays were carried out with a broad array of anthocyanin and other flavonoid substrates. We demonstrate that this enzyme carries out 3′, 5′-*O*-methylation of anthocyanins and flavonol compounds *in vitro*, which are known to be present in grape berries, with a preference for glycosylated substrates. The highest relative specific activity for the enzyme was found with delphinidin 3-*O*-glucoside as substrate. The enzyme is not able to methylate flavan type skeletons with chiral centers, such as either catechins or dihydroquercetin. The enzyme showed negligible specific activity for caffeoyl-CoA, compared to flavonol and anthocyanin substrates. Phylogenetic analysis of the *O*-methyltransferase suggests that it may be a member of a distinct subclass of Type 2 bivalent metal-dependent S-adenosylmethionine *O*-methyltransferases.

1. Introduction

Red grapes (*Vitis* spp.) and their fermentation products are rich sources of flavonoids that have important organoleptic and health-promoting properties. Anthocyanins impart red, blue, and purple coloration to grapes and wines, whereas flavonols in the grape exocarp (berry skin tissue) contribute to bitter taste, as well as to the stabilization of wine color through co-pigmentation with anthocyanins (Boulton, 2001). Certain anthocyanins and flavonoids were suggested to prevent the occurrence of skin cancer or act as protectants against blood and arterial diseases (Lila, 2004). Red wine anthocyanins have been shown to be absorbed by the human gastrointestinal tract into the circulatory system as intact glycosides (de Pascual-Teresa and Sanchez-Ballesta, 2008; Garcia-Alonso et al., 2009). The colorful anthocyanins are also important for the attraction of foraging animals and subsequent seed dispersal (Schaefer et al., 2008).

Grape berry growth follows a double sigmoidal curve. The onset of ripening (termed 'veraison' by viticulturists) marks the beginning of the second stage of growth when berries begin to soften and increase in size due to rapid cell enlargement. The sugar content of the berry increases rapidly and acidity decreases. During ripening initiation, the exocarp loses chlorophyll and begins to synthesize and accumulate phenolic compounds via the flavonoid pathway that are responsible for the development of characteristic colors, yellow-gold (flavonols), red (cyanidin-type anthocyanins), and blue to purple (delphinidin-type anthocyanins) (Fig. 1) (Watson, 2003). Flavonoid compounds all share the same basic skeleton, the flavan-nucleus, having two aromatic rings with six carbon atoms (rings A and B), connected by a heterocycle including three carbon atoms (ring C) (Fig. 1). Modifications of the central C-ring determine the specific structural class, such as flavanones, isoflavones, flavones, flavonols, flavanols, and anthocyanins. *Vitis* spp. berry exocarp does not contain pelargonidin-type anthocyanins, but grape cultivars accumulate diverse delphinidin- and cyanidin-type anthocyanins (Boss et al., 1996b). Flavonoids and anthocyanidins with a free hydroxyl group at the 3 position of the heterocyclic C-ring are unstable under physiological conditions and generally not found in nature (Forkmann and Heller, 1999). The enzyme, UDP-glucose:flavonoid 3-*O*-glucosyltransferase (3GT, EC 2.4.1.115), efficiently transfers a glucose moiety from

* Corresponding author. Address: 241-2205 East Mall, Vancouver, B.C., Canada V6T 1Z4. Tel.: +1 604 822 5708; fax: +1 604 822 5143.
E-mail addresses: jlucker@gmail.com (J. Lücker), stefan.martens@iasma.it (S. Martens), stlund@interchange.ubc.ca (S.T. Lund).
[1] Present address: School of Biological Sciences, 427 John Hines Building (62), The University of Queensland, St. Lucia, Qld 4072, Australia.

0031-9422/$ - see front matter Crown Copyright © 2010 Published by Elsevier Ltd. All rights reserved.
doi:10.1016/j.phytochem.2010.05.027

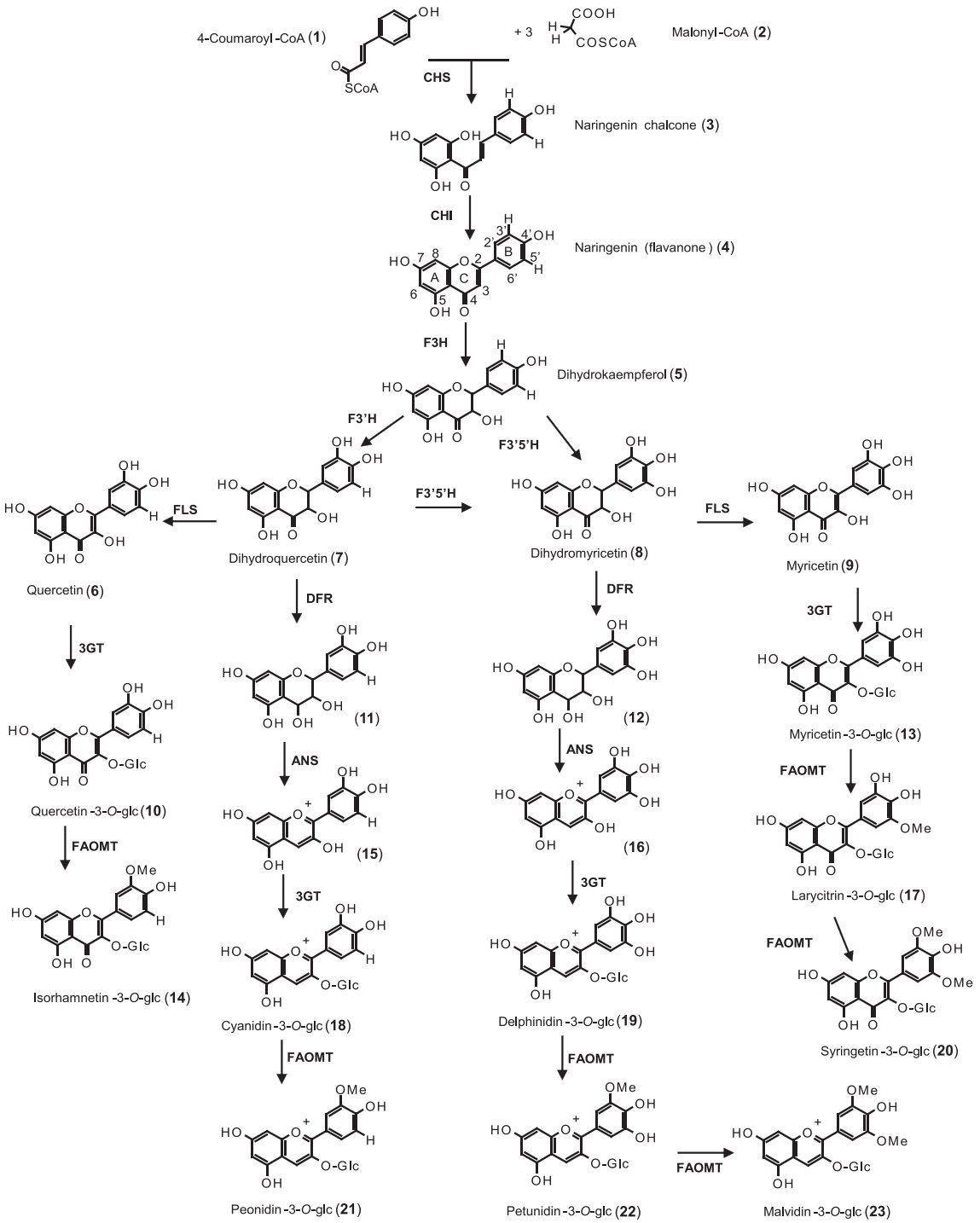

Fig. 1. The flavonoid biosynthesis pathway and structures of compounds found in *V. vinifera* berries. Branch pathways to proanthocyanidins as well as additional glycosylated and acylated anthocyanins and flavonoids are not shown. glc: glucoside.

UDP-glucose to position 3 of the C-ring, promoting stabilization. The expression of transcripts encoding 3GT coincides with the accumulation of anthocyanins in the exocarp of red grapes at ripening initiation (Boss et al., 1996a,b; Ford et al., 1998). Activity of native UDP-glucose:cyanidin 3-*O*-glucosyltransferase isolated from grape cell suspension cultures, as with the heterologously expressed enzyme, was highest with delphinidin (**16**) and cyanidin (**15**), and much lower with their respective methylated forms (Do et al., 1995; Ford et al., 1998). *O*-methylation of anthocyanins at available hydroxyl groups at the 3′ and 5′ positions of the B-ring was shown to be more efficient with cyanidin 3-*O*-glucoside (**18**) as substrate than with the respective aglycone by enzyme assays using a native *O*-methyltransferase (OMT) partially purified from *V. vinifera* cell cultures (Bailly et al., 1997). It is likely, therefore, that in *V. vinifera*, the *O*-methylation step occurs after the glycosylation step in the pathway, as shown in Fig. 1.

Expression of a putative transcript for this anthocyanin *O*-methyltransferase activity was first discovered when a caffeoyl-CoA *O*-methyltransferase (*cCoAomt*)-like gene was found to be one of nine transcripts consistently up-regulated coincident with the occurrence of red pigmentation in berry exocarp (Ageorges et al., 2006). Subsequently, transcript (Castellarin and Di Gaspero,

2007; Lund et al., 2008) and protein (Lücker et al., 2009) accumulation likely representing the same OMT was also correlated with the expression of other flavonoid pathway genes or proteins and the onset of ripening in several *V. vinifera* cultivars. The *omt* transcript abundance and degree of anthocyanin methylation was highest in berries of grape cultivars with darker hues (Castellarin and Di Gaspero, 2007). Despite the availability of these data, the isolation of a functional full length cDNA for the respective OMT and its biochemical characterization have not been completed thus far.

Methyltransferases were recently divided into three different families based upon a combination of sequence alignments and structural studies (Noel et al., 2003). The three types show differences in structural folding. Catalysis is influenced by a different organization of active site residues. Type 1 methyltransferases generally methylate hydroxyl moieties of phenylpropanoids, like caffeic acid (Fig. 4F, **30**). Type 2 methyltransferases are found in all lignin producing plants and are specific for coenzyme A-derivatized phenylpropanoid compounds. Bacterial macrolide biosynthesis methyltransferases and mammalian catechol OMTs are also related to these (Noel et al., 2003). Type 3 methyltransferases have been named the SABATH family of methyltransferases and consist mainly of enzymes converting carboxylic acids to methyl ester derivatives (D'Auria et al., 2003; Noel et al., 2003). Type 2 S-adenosylmethionine (SAM) and bivalent metal ion cofactor-dependent enzymes are usually involved in lignin biosynthesis and are specific for caffeoyl-CoA (Fig. 4H, **32**) and 5-hydroxyferuloyl-CoA. Recently, a new subclass was shown to have preference for flavonoids, as well as these respective phenylpropanoids as substrates (Ibdah et al., 2003). We report here on the identification and functional characterization of a SAM- and Mg-dependent OMT activity that prefers flavonol- and anthocyanidin-glycosides as substrates and performs methylation at the 3′ and 5′ positions on the B-ring of the flavan skeleton; however, in contrast to the previously characterized promiscuous enzymes of the second Type 2 OMT subclass (Ibdah et al., 2003), this Type 2 OMT shows only negligible activity with caffeoyl-CoA (**32**) tested as a substrate.

2. Results

2.1. Identification of faomt and relatedness to other sequences by phylogeny

Correlation of gene and protein expression patterns with the accumulation of methylated anthocyanins in grape exocarp identified a predicted *omt* sequence, Genbank ID: ABQ02272, from *V. vinifera* cv. Nebbiolo (Castellarin and Di Gaspero, 2007; Lücker et al., 2009). A tblastn search of Cabernet Sauvignon berry expressed sequence tags (ESTs) (Peng et al., 2007) with ABQ02272 revealed a single clone with 100% sequence identity, which had a predicted 48 amino acid N-terminal extension, as do the most similar paralogs identified in the Pinot Noir genome sequence data, Genbank IDs: CAO66180, CAO66182, and CAO66184 (The French-Italian Consortium for Grapevine Genome Characterization, 2007). The 1001 bp full length cDNA from Cabernet Sauvignon that we designated '*faomt*' for 'flavonol and anthocyanin 3′, 5′-*O*-methyltransferase', contains an open reading frame of 708 bp which encodes a protein of 235 amino acids, having a predicted molecular mass of 26.4 kDa and a theoretical isoelectric point of 5.84. The Genbank ID for this nucleotide sequence is HM142924.

The closest ortholog to *faomt* in the nr database was a *Plantago major cCoAomt* (Genbank ID: CAJ43712) with 70.3% identity, thus far without determined biochemical function. The closest characterized *omt* to *faomt* was found to be a *Mesembryanthemum crystallinum* phenylpropanoid and flavonoid *omt* (*pfomt*; AY145521) with 54.9% identity that was proposed to form a second subclass within the family of Type 2 OMTs (Ibdah et al., 2003; Noel et al., 2003).

In a search for other *V. vinifera* paralogs that were closely related to *pfomt* or *faomt* in the Pinot Noir genome, three additional distinct Type 2 *cCoAomts* were identified. For genomic clone, CAO65398, with 67.1% identity to *pfomt* and 51.7% to *faomt*, an EST was identified from *V. shuttleworthii* (CV093856) but no orthologous ESTs were found from *V. vinifera*. CAO69794 with 60.8% identity to *pfomt* and 48.3% to *faomt* was found as an EST in Cabernet Sauvignon petiole tissue (CF517412). For the genomic clone CAO65399 (65.8% identity to *pfomt*, 52.5% to *faomt*), a corresponding *Vitis* EST could not be retrieved from Genbank and was not investigated further. For additional identity percentages between related sequences, see Supplementary material Table S1.

Phylogeny analysis of these sequences, described above, in combination with representatives of Type 1 OMTs showed that FAOMT is a Type 2 methyltransferase family member (Fig. 2). FAOMT falls outside the subclade of the true caffeoyl-CoA methyltransferases, containing a characterized *Vitis cCoAomt* paralog, Genbank ID: Z54233 (Busam et al., 1997; Ibdah et al., 2003), and does not form a branch in the second subclade of promiscuous Type 2 OMTs (Ibdah et al., 2003). Fig. 2 shows that the latter subclade with PFOMT does include the two newly identified expressed paralogs from *Vitis* species.

2.2. FAOMT amino acid alignment

The conservation between the *Vitis* FAOMT and other Type 2 OMTs is shown in an amino acid alignment (Fig. S1). The organization and number of the consecutive α-helix and β-sheet domains is conserved for FAOMT (Kopycki et al., 2008). The amino acids responsible for binding the SAM/SAH molecules and the bivalent metal ion are mostly conserved between FAOMT and the biochemically characterized Type 2 OMTs, *Sl*-OMT, *Mc*-PFOMT, *At*-OMT, *Vv*-CCoAOMT, *Ms*-CCoAOMT, and *Os*-08g0498100 (rice OMT15). The most striking differences between FAOMT and other OMTs are that the FAOMT has a shorter N-terminal region, and a more polar insertion loop domain. The CCoAOMTs involved in lignin biosynthesis have a conserved Arg-206, which was suggested to interact with the negatively charged 3′-phosphate group of the adenosine 3′-5′-diphosphate moiety of CoA (Ferrer et al., 2005); this residue is not present in PFOMT and FAOMT. As was determined by crystallography for iceplant PFOMT and the *Medicago sativa* CCoAOMT, the variable N-terminal region (Fig. S1) is likely involved in determining the position specificity and the kinetic properties of these enzymes; for PFOMT, in particular, it was postulated that this may affect the specificity for flavonoid substrates (Ferrer et al., 2005; Kopycki et al., 2008; Vogt, 2004). The N-terminal region of FAOMT is shorter and consists of four polar serines followed by two positively charged amino acids that are not conserved in PFOMT and SlOMT, but are present in the CCoAOMTs. The insertion loop domain indicated in Fig. S1 shows that FAOMT has more polar negatively charged amino acids (D, E) in the middle of this domain than PFOMT and its related enzymes. The FAOMT insertion loop domain shows even lower conservation with that of CCoAOMT from *M. sativa* than with that of PFOMT. The *M. sativa* insertion loop domain contains fewer charged amino acids but has, for instance, three nonpolar neutral prolines that are not conserved in FAOMT. The amino acid side chains of Tyr-51, Trp-184, and Phe-198 in PFOMT that were predicted to be involved in sandwiching the quercetagetin and quercetin (**6**) aromatic moieties and locating the hydroxyl groups to be methylated on the flavonoid molecule closely to the SAM (Kopycki et al., 2008) are conserved, but the Tyr-51 is replaced by a leucine in FAOMT, similar to the isoleucine in the *M. sativa* CCoAOMT, although another Tyr is present three amino acids upstream from the Leu.

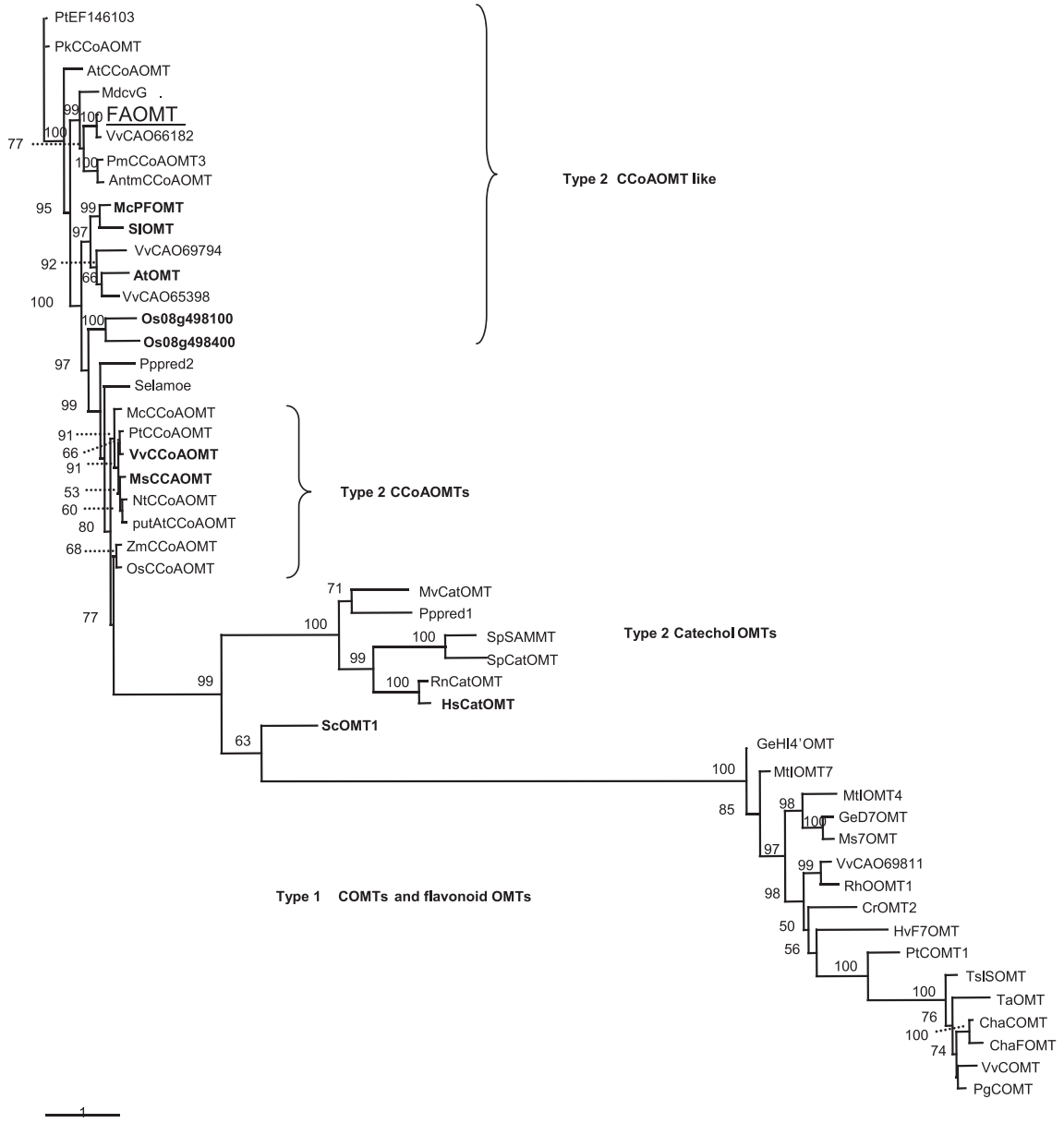

Fig. 2. Phylogenetic analysis of FAOMT from *V. vinifera* with other OMTs. Bootstrap values with a minimum of 50% for maximum likelihood are displayed. Maximum likelihood values represent percentages of 500 γ-corrected replicates (log L = −18792.64) analyzed using Phyml. FAOMT is underlined and displayed in a larger font. Enzymatically characterized Type 2 OMTs are displayed in bold font. Type 1 OMTs (Noel et al., 2003): RhOOMT1 *Rosa hybrida* orcinol OMT (AF502433), HvF7OMT *Hordeum vulgare* flavonoid 7-*O*-OMT (X77467), PtCOMT1 *Pinus taeda* caffeic acid OMT (COMT) (U39301), CrOMT2 *Catharanthus roseus* COMT2 (AY127568), ChaCOMT *Chrysosplenium americanum* COMT (U16793), ChaFOMT *C. americanum* 3′, 5′ flavonoid OMT (U16794), TsISOMT *Thalictrum tuberosum* isoquinoline OMT (AF064696), TaOMT2 *Triticum aestivum* 3′,4′,5′ flavonoid OMT (DQ223971), MtIOMT4 *Medicago truncatula* isoflavonoid OMT (DQ419912), MtIOMT7 *M. truncatula* isoflavonoid OMT (DQ419914), GeHI4′OMT *Glycyrrhiza echinata* 2′,7,4′-hydroxyflavonone 4′-OMT (AB091684), GeD7OMT *G. echinata* 7-OMT (AB091685), Ms7OMT *Medicago sativa* isoflavone 7-OMT (U97125), PgCOMT *Populus* × *generosa* COMT (M73431), VvCOMT *V. vinifera* COMT (AF239740), VvCAO69811 *V. vinifera* PN40024 genomic DNA derived, related to IOMT. Type 2 OMTs: MsCCoAOMT *M. sativa* (U20736), McCCoAOMT *Mesembryanthemum crystallinum* CCoAOMT (AF053553), NtCCoAOMT *Nicotiana tabacum* CCoAOMT (Z82982), putAtCCoAOMT *Arabidopsis thaliana* putative CCoAOMT (NM_119566), PtCCoAOMT *Populus trichocarpa* CCoAOMT (AJ224894), VvCCoAOMT *V. vinifera* CCoAOMT (Z54233), ZmCCoAOMT *Zea mays* CCoAOMT (AJ242980), OsCCoAOMT *Oryza sativa* cv. japonica CCoAOMT (NM_001063445 Os06g0165800), MvCatOMT *Mycobacterium vanbaalenii* PYR-1 (Mvan3280), Pppred1 *Physcomitrella patens* subsp. Patens predicted protein 1 (XM_001766915), SpSAMMT *Schizosaccharomyces pombe* SAM-dependent OMT (NM_001020945), SpCatOMT *S. pombe* probable catechol OMT (SPBC119), RnCatOMT *Rattus norvegius* catechol OMT (M60753), HsCatOMT *Homo sapiens* catechol OMT (NM_007310), Sc-OMT1 *Streptomyces coelicolor* A3(2) (SCO2338), Pppred2 *P. patens* subsp. Patens predicted protein 2 (XM_001754959), Selamoe: *Selaginella moellendorfii* EST sequence (FE444786), Os08g498100; *O. sativa* CCoAOMT ROMT15 (Os08g498100), Os08g498400; *O. sativa* CCoAOMT ROMT17 (Os08g498400), AtCCoAOMT *A. thaliana* CCoAOMT (NM_105468), PtEF146103 *P. trichocarpa* unknown (EF146103), PkCCoAOMT *Populus kitakamiensis* CCoA 3-OMT (AB000408), MdcvG *Malus x domestica* cv. Gala EST sequence (EB129882), PmCCoAOMT *Plantago major* (first 22 N terminal amino acids removed from AM159091), AntmCCoAOMT *Anthirrinum majus* EST sequence (AJ792459), FAOMT *V. vinifera* cv. Cabernet Sauvignon flavonoid and anthocyanin methyltransferase, VvCAO66182 *V. vinifera* PN41004 genomic DNA derived, McPFOMT *M. crystallinum* phenylpropanoid and flavonoid OMT (AY145521), SlOMT *Stellaria longipes* CCoAOMT (L22203), AtOMT *A. thaliana* CCoAOMT-like (AY087244), VvCAO65398; *V. vinifera* PN41004 genomic DNA derived, VvCAO69794; *V. vinifera* PN41004 genomic DNA derived.

2.3. Analysis of relative expression by real time RT-PCR

The four representative genes from the Type 2 *omt* family were analyzed for expression in different tissues along ripening using real time RT-PCR (Fig. 3). In the exocarp, *faomt* transcripts began accumulating at ripening initiation and peaked shortly thereafter, followed by a gradual decrease as the berry matured (Fig. 3A). Expression in other tissues was lower, but strongest in tendrils

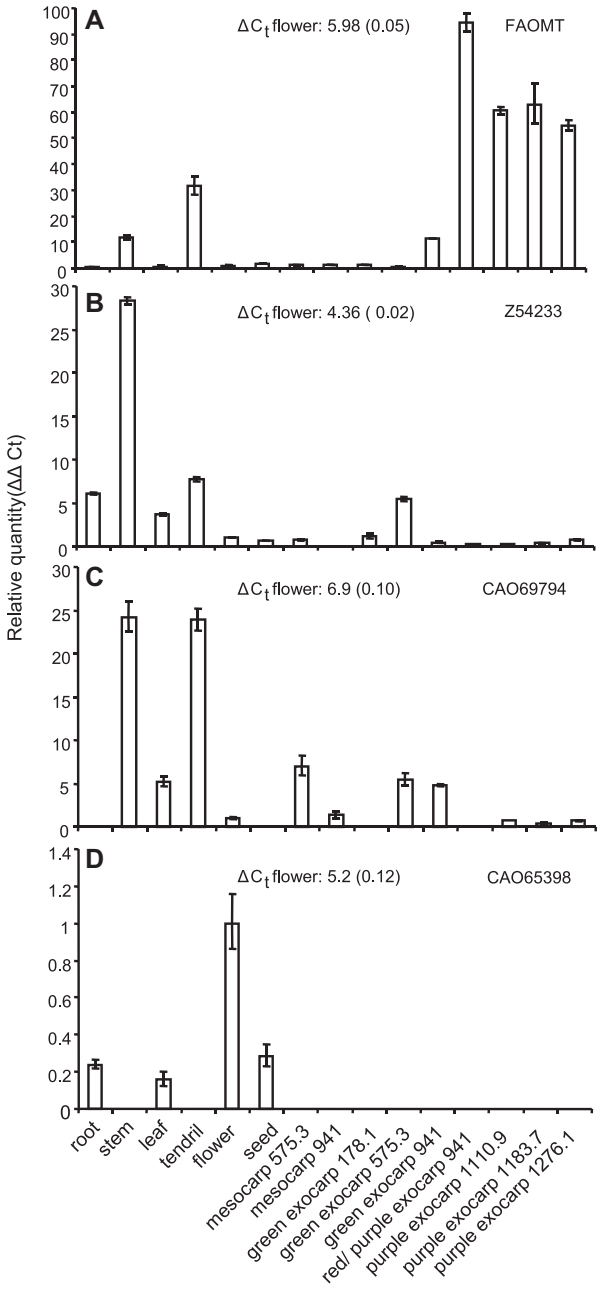

Fig. 3. Relative expression of the different Type 2 *V. vinifera O*-methyltransferases in grape tissues. Expression is displayed as relative quantity ($\Delta\Delta Ct$) with flower tissue as the calibrator sample and glyceraldehyde 3-phosphate dehydrogenase as the reference gene. (A) FAOMT flavonol and anthocyanin *O*-methyltransferase, (B) Z54233 *Vitis vinifera* previously characterized true caffeoyl-CoA *O*-methyltransferase (Busam et al., 1997), (C) CAO69794 genomic clone of putative type 2 OMT and detected as an expressed sequence tag in Cabernet Sauvignon petiole tissue (CF517412), (D) CAO65398 genomic clone of putative type 2 OMT and detected as an expressed sequence tag in *V. shuttleworthii* (CV093856). Flower ΔCt for the different genes are displayed in each panel. Exocarp and mesocarp stages are defined by growing degree days (GDD), which are calculated by taking the average of the daily high and low temperature of each day compared to a baseline (10 °C). Fifty percent ripening initiation in the 2003 season was just prior to 941 GDD.

and stems. The true *cCoAomt* from *V. vinifera* (Z54233) (Busam et al., 1997) was mainly expressed in the stem and to a lesser extent in the tendril, root, leaf, and exocarp tissues before ripening initiation (Fig. 3B). Of the two other *V. vinifera* genes that grouped with *pfomt* in the phylogenetic tree, CAO69794 was expressed most highly in stem and tendril, and lower in leaf and green berry stages (Fig. 3C). Fig. 3D shows that the CAO65398 transcript was detectable in flower, root, leaf, and seed.

2.4. Enzyme activity assays

The purified recombinant FAOMT (Fig. S2) was used in enzyme assays with an array of relevant substrates with different functional groups and chirality (Fig. 4). A pH optimum of 8.5 was determined for FAOMT using cyanidin 3-*O*-glucoside (**18**) and quercetin 3-*O*-glucoside (**10**) as substrates. FAOMT activity was tested in four different buffers so that the pH ranged from 2.9 to 9.4. Activity was detected at pH 6.0 and higher (Fig. S3). The substrate conversion rate was maximal close to 49 °C, with half maximal conversion rate around 40 °C, showing a sharp decline at temperatures higher than 51 °C (Fig. S4). The pH optimum curve became sharper as the temperature of the assay was adjusted closer to the point of maximal conversion rate, and half maximal activity was detected at pH 8 and pH 8.8 (Fig. S5).

The enzyme was dependent on the addition of a metal cofactor with only traces of product detected in the absence of $MgCl_2$. This was likely due to traces of bivalent metals in the assay buffer. Optimal activity was seen with $MgCl_2$ used at a concentration of 7 mM. With the addition of EDTA as a metal chelator to the assay, no activity was detected (Fig. 5). FAOMT also required the addition of S-adenosyl-methionine (SAM or AdoMet) as a methyl donor.

Substrates tested		Side chains			
		R3	R5	$R_{3'}$	$R_{5'}$
Delphinidin (**16**)	A	OH	OH	OH	OH
Delphinidin 3-*O*-glc (**19**)	A	*O*-glc	OH	OH	OH
Cyanidin (**15**)	A	OH	OH	OH	H
Cyanidin 3-*O*-glc (**18**)	A	*O*-glc	OH	OH	H
Petunidin (**24**)	A	OH	OH	OMe	OH
Petunidin 3-*O*-glc (**22**)	A	*O*-glc	OH	OMe	OH
Pelargonidin 3-*O*-glc (**25**)	A	*O*-glc	OH	H	H
Cyanidin 3-*O*-rut (**26**)	A	*O*-rut	OH	OH	H
Cyanidin 3,5-di-*O*-β-glc (**27**)	A	*O*-glc	*O*-glc	OH	H
Quercetin (**6**)	B	OH	OH	OH	H
Quercetin 3-*O*-glc (**10**)	B	*O*-glc	OH	OH	H
Myricetin (**9**)	B	OH	OH	OH	OH

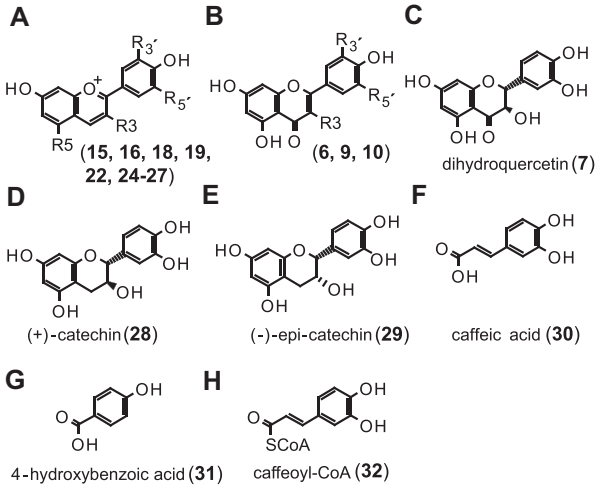

Fig. 4. Presentation of structure skeletons tested as substrates for FAOMT. (A) Anthocyanidin and anthocyanidin-glucosides with different R groups representing various skeleton side chains. (B) Flavonols and flavonol glucosides, R groups representing various skeleton side chains. (C)–(E) Flavonoid skeletons with chiral centers. (C) dihydroquercetin (**7**), (D) (+)-catechin (**28**), (E) (−)-epi-catechin (**29**), (F) caffeic acid (**30**), (G) 4-hydroxybenzoic acid (**31**), (H) caffeoyl-CoA (**32**). glc: glucoside, rut: rutinoside.

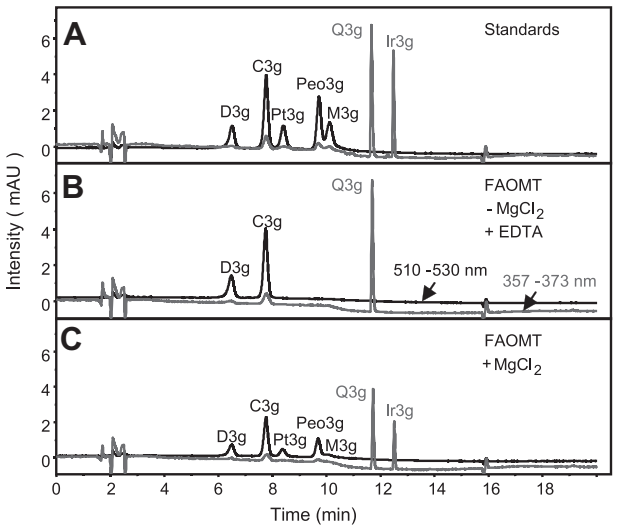

Fig. 5. LC–DAD chromatograms of multiple substrate conversion by FAOMT. Absorbance (mAU) is indicated on the left. (A) Ten μM of authentic standards treated under assay conditions. (B) Ten μM each of delphinidin 3-*O*-glucoside (**19**, D3 g), cyanidin 3-*O*-glucoside (**18**, C3 g) and quercetin 3-*O*-glucoside (**10**, Q3 g) added simultaneously as substrates to be converted by FAOMT (350 ng) with addition of EDTA in the buffer and without MgCl2 added. (C) Same amounts of substrates added to the assay as in (B), but with addition of MgCl2 and without EDTA. Assays were incubated at 35 °C for 10 min. Other peaks indicated are: Pt3 g: petunidin 3-*O*-glucoside (**22**), Peo3 g: peonidin 3-*O*-glucoside (**21**), M3 g: malvidin 3-*O*-glucoside (**23**), Ir3 g: isorhamnetin 3-*O*-glucoside (**14**).

Enzyme assays were carried out under saturating concentrations of 0.5 mM SAM.

After initial experiments where relative specific activity was compared for all substrates at 49 °C, we detected possible degradation of some of the substrates at this temperature in addition to their methylation, as the resulting loss in substrate did not account for the increase in product formed. Eleven different flavonoid substrates and products were simultaneously tested for stability under assay conditions using two different lengths of incubation at eight different temperatures (Fig. S6). Results showed that relative to the 0 °C control, the flavonol glycosides were relatively stable even at 55 °C, whereas the flavonol aglycones were substantially degraded after 18 min incubation at 55 °C. The cyanidin-derived glycosides showed higher temperature stability than the delphinidin-derived glycosides. Methylated anthocyanins were more stable under assay conditions than their non-methylated analogs. Delphinidin 3-*O*-glucoside (**19**) was the least stable but was 82% intact after 18 min incubation at 35 °C (Fig. S6).

At 35 °C, FAOMT had the highest relative specific activity with delphinidin 3-*O*-glucoside (**19**) (Table 1). There was no significant difference in specific activity with cyanidin 3-*O*-glucoside (**18**) and cyanidin 3-*O*-rutinoside (**26**). The relative activity measured with cyanidin 3, 5-di-*O*-*β*-glucoside (**27**), however, was only 55%. Relative specific activity rates for other substrates are shown in Table 1. Myricetin (**9**) and quercetin (**6**), which also have three or two vicinal hydroxyl groups on the B-ring of the flavan molecule, were methylated as well. Quercetin (**6**) is converted less efficiently than its glucoside (**10**) (Table 1). The anthocyanidins were also converted to the predicted 3′- and 5′-methylated products, as identified by their respective authentic standards, but these aglycones were highly unstable and their relative specific activities could not be determined (Table 1).

Although the flavonols, flavonol glucosides, and anthocyanins were all converted to their expected 3′- and 3′, 5′-methylated products by FAOMT, dihydroquercetin (**7**), caffeic acid (**30**), and the chiral flavanols, catechin (**28**) and epi-catechin (**29**), were not methylated by this enzyme, not even when using increased protein amounts of up to 500 ng and longer incubation times up to 30 min (Fig. 4). Caffeoyl-CoA (**32**) methylation could not be detected under the linear conditions for the flavonol and anthocyanin substrates, but increased protein amounts and incubation time did result in conversion to feruloyl-CoA. Substrates with vicinal hydroxyl groups on the B-ring of the flavan structure and lacking chiral centers were converted by FAOMT. Substrates with vicinal hydroxyl groups on the A ring were not tested. Pelargonidin 3-*O*-glucoside (**25**) and 4-hydroxybenzoic acid (**31**), both used as controls to

Table 1
Substrate conversion by FAOMT. Specific activity of FAOMT at 35 °C with 4 μM cyanidin-3-*O*-glucoside (**18**) substrate of 10.25 (SE = 0.73) nkatal mg^{-1} His-tag purified protein was set to 100%.

Substrate	Rt (*m*/*z* substrate)	Rt (*m*/*z* product)	Authentic standard product(s) Rt (*m*/*z*)	Reaction type	Relative specific activity (std. dev.)
Cyanidin 3-*O*-glucoside (**18**)	7.7 (449)	9.64 (463)	Peonidin 3-*O*-glucoside (**21**) 9.64 (463)	3′-*O*-methylation	100 (12)
Delphinidin 3-*O*-glucoside (**19**)	6.4 (465)	8.3 (479), 10.0 (493)	Petunidin 3-*O*-glucoside (**22**) 8.3 (479), malvidin 3-*O*-glucoside (**23**) 10.0(493)	3′,5′-*O*-methylation	169 (18)
Petunidin 3-*O*-glucoside (**21**)	8.3 (479)	10.0 (493)	Malvidin 3-*O*-glucoside (**23**) 10.0 (493)	5′-*O*-methylation	52 (5)
Quercetin 3-*O*-glucoside (**10**)	11.64 (465)	12.45 (479)	Isorhamnetin 3-*O*-glucoside (**14**), 12.45 (479)	3′-*O*-methylation	76 (5)
Quercetin (**6**)	13.8 (303)	15.15 (317)	Isorhamnetin 15.15 (317)	3′-*O*-methylation	40 (11)
Myricetin (**9**)	12.5;(319)	13.9 (333), 15.1 (347)	Not used	Likely 3′, 5′-*O*-methylation	nd
Cyanidin aglycone (**15**)	10.7 (287)	11.9 (mostly 285, some 301)	Peonidin 11.9 (301)	3′-*O*-methylation, then oxygen loss in MS	nd
Delphinidin aglycone (**16**)	10.0 (303)	11.3 (317), 11.75 (349), 12.1 (331), 12.1 (315, most abundant)	Petunidin (**24**) 11.3 (317), malvidin 12.1 (331)	3′, 5′-*O*-methylation, water addition, loss of oxygen in MS	nd
Petunidin aglycone (**24**)	11.3 (317)	11.75 (349), 12.1 (315)	Malvidin 12.1 (331)	5′-*O*-methylation, water addition, loss of oxygen in MS	nd
Cyanidin 3-*O*-rutinoside (**26**)	8.3 (595)	10.07 (609)	Not used	Likely 3′-*O*-methylation	119 (11)
Cyanidin-3,5-di-*O*-*β*-glucoside (**27**)	5.3 (611)	6.94 (625)	Not used	Likely 3′-*O*-methylation	55 (9)

(+)-Catechin (**28**), caffeic acid (**30**), (−)-epi-catechin (**29**), 4-hydroxybenzoic acid (**31**), and pelargonidin 3-*O*-glucoside (**25**) were not converted by FAOMT. Caffeoyl-CoA (**32**) conversion to feruloyl-CoA could not be detected under the above conditions. Dihydroquercetin (**7**) was not methylated but most likely isomerized, forming a second peak with identical *m*/*z* 303). Rt = retention time in min., *m*/*z* = $[M]^+$.

check for possible methylation on the 4′ position, remained unaltered.

Fig. 5 shows UV-DAD LC chromatograms of assays where three substrates common to grape berries, delphinidin 3-*O*-glucoside (**19**), cyanidin 3-*O*-glucoside (**18**), and quercetin 3-*O*-glucoside (**10**) were presented to the enzyme simultaneously in a competition assay. The chromatograms showed that the retention times of product authentic standards were identical to retention times of the products produced by FAOMT. The *m*/*z* values for the parent ions were also identical (Table 1). From integrations of the peak areas, it was verified that delphinidin 3-*O*-glucoside (**19**) was converted the most in this multi-substrate assay, followed by cyanidin 3-*O*-glucoside (**18**), and then quercetin 3-*O*-glucoside (**10**).

Enzyme kinetic data were determined using quercetin 3-*O*-glucoside (**10**) and cyanidin 3-*O*-glucoside (**18**) as substrates at 49 °C. The affinity (K_m) of FAOMT for quercetin 3-*O*-glucoside (**10**) was 3-fold greater than for cyanidin 3-*O*-glucoside (**18**). The turnover number (K_{cat}) for cyanidin 3-*O*-glucoside (**18**) was 3-fold higher than for quercetin 3-*O*-glucoside (**10**), resulting in no significant difference in catalytic efficiency (Table 2). The specific activity at 49 °C using 4 μM cyanidin 3-*O*-glucoside (**18**), which was also used in the substrate efficiency determination experiments (Table 1), was 28.8 nkatal per mg enzyme. For quercetin 3-*O*-glucoside (**10**), the relative specific activity to cyanidin 3-*O*-glucoside (**18**) was 66.7% at this temperature, which is a similar ratio as what was found by the experiment conducted at the lower temperature of 35 °C.

3. Discussion

We conclude that FAOMT methylates flavonol, anthocyanin, and flavonol-glycoside substrates in the exocarp of grape. Expression of *faomt* (Ageorges et al., 2006; Castellarin and Di Gaspero, 2007; Castellarin et al., 2006; Lund et al., 2008) and its protein (Lücker et al., 2009) are closely temporally and spatially correlated with the accumulation of these methylated compounds. The two expressed Type 2 *omts* present in the grape genome that are more closely related to *pfomt* than to *faomt* showed an expression pattern more like that of the true *cCoAomt* of *V. vinifera* than *faomt*, and are likely not involved in the methylation of anthocyanins in grape exocarp.

The high specific activity of FAOMT with the glycosides tested, the low K_ms, and the high catalytic efficiency ($K_{cat}K_m^{-1}$) compared with the lower specific activity for the aglycone quercetin (**6**) provide further evidence to place FAOMT activity after that of 3GT in the anthocyanin pathway, supporting the current hypothesis held for *V. vinifera* (Bailly et al., 1997; Castellarin and Di Gaspero, 2007; Do et al., 1995; Ford et al., 1998). The highest specific activity for FAOMT was found for the most labile anthocyanin substrate, delphinidin 3-*O*-glucoside (**19**), which is converted by this enzyme in two subsequent methylation steps to malvidin 3-*O*-glucoside (**23**) (Jackman and Smith, 1996; Sroka, 2005). It is not surprising, then, that the more stable 3′, 5′-methylated malvidin 3-*O*-glucoside (**23**) is the most abundant anthocyanin in most red *V. vinifera* grapes (Mori et al., 2007; Wang et al., 2003).

In Type 2 *O*-methyltransferases, the N-terminal region and an insertion loop domain near the C-terminus are important for substrate binding and site of methylation, as was shown by domain swapping experiments between a true *M. sativa* CCoAOMT and the iceplant PFOMT (Ferrer et al., 2005; Kopycki et al., 2008). For CCoAOMT, the insertion loop domain was predicted to provide a scaffold for the CoA moiety of the caffeoyl-CoA (**32**) during catalysis (Ferrer et al., 2005). The N-terminal region in FAOMT is shorter than the N-terminal region in PFOMT and in most other OMTs. A shorter N-terminal region has been suggested to lower the specificity for caffeoyl-CoA (**32**) and caffeic acid (**30**) (Vogt, 2004). Since the expression pattern for *faomt* was distinct from that of the true *V. vinifera cCoAomt* (Busam et al., 1997), FAOMT is not likely to function in the conversion of caffeoyl-CoA (**32**), which is in agreement with the negligible activity found here. The insertion loop domain in FAOMT is more polar and negatively charged in relation to that in PFOMT, perhaps providing a manifold for the glycosidic forms and positively charged anthocyanins preferred by the FAOMT enzyme compared to caffeoyl-CoA (**32**). The flavonol, quercetin 3-*O*-glucoside (**10**), was also converted by the iceplant PFOMT enzyme, but the PFOMT showed higher relative specific activity, thus higher preference for its aglycone, whereas caffeoyl-CoA (**32**) was preferred by this enzyme in an equal manner as to quercetin (**6**) (Ibdah et al., 2003).

Type 1 and Type 2 *O*-methyltransferases share some substrate specificities, as both of these families have been shown to convert flavonoid aglycones in plants (Cacace et al., 2003; Ibdah et al., 2003). CrOMT2 from *Catharanthus roseus*, an enzyme belonging to the Type 1 family, does not accept phenylpropanoids as substrates, only flavonoids. While only non-glycosylated flavonoids were tested, the enzyme not only could accept the flavonols, myricetin (**9**) and quercetin (**6**), as substrates but also the dihydroflavonols, dihydroquercetin (**7**) and dihydromyricetin (**8**) (Cacace et al., 2003). These latter ones are compounds with the B-ring protruding out of the plane in relation to the heterocycle, connected to the A-ring of the flavan molecule. This is in contrast to FAOMT which cannot methylate these types of compounds. Whether this is unique to FAOMT or common to Type 2 OMTs is not known, since the iceplant PFOMT was not tested for activity with dihydroquercetin (**7**) (Ibdah et al., 2003). Although these authors did detect some activity for the recombinant PFOMT using another chiral flavonoid, catechin (**28**), as substrate, this activity was absent for the native enzyme (Ibdah et al., 2003). The recombinant FAOMT enzyme did not show activity with catechins (**28, 29**), either.

Considering the high pH optimum of 8.5 and the minimum pH of 6.0 for FAOMT activity, the enzyme is likely localized to the cytoplasm, possibly associated with the endoplasmic reticulum along with other components of the flavonoid biosynthetic pathway (Hrazdina and Jensen, 1992; Poustka et al., 2007; Winkel-Shirley, 1999). The pH of the cytoplasm was shown to be around pH 7 in other plant species (Felle, 2005). The pH optimum for FAOMT of 8.5 is similar to the pH optimum of the partially purified native *V. vinifera* cyanidin 3-*O*-methyltransferase, although a broader pH range from 7.75 to 9.75 was reported (Bailly et al., 1997).

True Type 2 CCoAOMTs have been shown to convert certain flavonol aglycones such as quercetin (**6**), although at a much lower rate than with PFOMT (Ibdah et al., 2003; Lukacin et al., 2004). This could indicate that the true CCoAOMTs and the more flavonoid-

Table 2
Kinetic properties of the purified His-tagged FAOMT. Linear assay conditions were performed under optimal temp. of 49 °C.

	km (μM)	V_{max} (nkatal mg^{-1})	K_{cat} (s^{-1})	K_{cat}/km (M^{-1} s^{-1})	V at 4 μM (nkatal mg^{-1})
Cyanidin 3-*O*-glucoside (**18**)	7.60, SE = 0.07	83.38, SE = 4.43	2.3825	313,487	28.8, SE = 0.8
Quercetin 3-*O*-glucoside (**10**)	2.70, SE = 0.05	31.17, SE = 1.3	0.8976	332,442	19.16, SE = 0.37

Specific activity at 4 μM substrate is given for comparison to the conversion at 35 °C in Table 1. Parameters were determined for product accumulation and calculated using calibration curves of products incubated under the same assay conditions.

specific methyltransferases share a common ancestor. It is interesting to note that the more ancient species, *Physcomitrella patens* and *Selaginella moellendorfii*, both possess at least one ortholog to the Type 2 caffeoyl-CoA methyltransferases, as obtained from EST database mining. These homologs do not group into any of the specific subclades, but show relatedness to all subclades of the Type 2 OMTs in the bootstrapped tree. Phylogenetic analysis of the FAOMT amino acid sequence showed that it grouped together with other uncharacterized Type 2 plant OMTs in a statistically significant, distinct group from the subclade containing the PFOMT and other characterized Type 2 OMTs. We suggest that FAOMT could be the first characterized enzyme of a third subclass of the Type 2 family of bivalent metal and SAM-dependent OMTs, based on FAOMT's high specific activity with glycosylated flavonols and anthocyanins, its separate phylogenetic assignment, distinctions in the active site domains, and its lack of significant activity with caffeoyl-CoA (**32**). The two other uncharacterized, low abundance *V. vinifera* CCoAOMT-like transcripts that are more closely related to PFOMT are perhaps more promiscuous like PFOMT and their occurrence in the grape genome could be an indication that these are ancestral forms of both the true CCoAOMT and FAOMT. This postulate is strengthened by the fact that orthologs in the ancient plant species show resemblance to all Type 2 subclasses in their insertion loop domain and by phylogenetic analysis.

A biological explanation for the maximal conversion rate of the enzyme at the high temperature of 49 °C that we determined for FAOMT may be that elevated ambient temperatures normally cause degradation of UV-protecting flavonols and anthocyanins, but methylation in addition to glycosylation can abate degradation, as we showed using a number of flavonoid standards. Further, the antioxidant capacity of anthocyanins has been suggested to be greater at higher temperatures as a means of protecting plants from excessive temperature injury and UV radiation damage (Shao et al., 2007). Although total anthocyanin content was reported to be lower at higher temperature conditions, the malvidin glycoside content in the grape exocarp was not affected (Mori et al., 2007). Cooling of sun exposed grapes resulted in increased total anthocyanin content of grapes in field experiments (Spayd et al., 2002). In warm climates, such as in many of the Australian wine growing regions, it was shown for Shiraz berries that heat induced the up-regulation of the *fls* gene, presumably underlying the accumulation of the more UV-protecting quercetin 3-*O*-glucoside (**10**) and isorhamnetin 3-*O*-glucoside (**14**) close to the end of the season (Downey et al., 2006, 2003). The abundance of these flavonol glucosides correlating with higher seasonal growing temperatures is in agreement with our finding that quercetin 3-*O*-glucoside (**10**) and isorhamnetin 3-*O*-glucoside (**14**) were the most stable compounds under high temperature conditions. FAOMT activity may have evolved in plant tissues containing high amounts of flavonoids in order to increase stabilization against oxidation and heat degradation.

4. Experimental

4.1. Plant material and real time RT-PCR

RNA isolation of plant tissues, cDNA synthesis, primer design, and real time RT-PCR analyses were performed essentially as previously described (Reid et al., 2006), but using Finnzymes DyNAmo™ HS SYBR® Green qPCR kit (www.Finnzymes.com) and ABI 7500 software v. 2.0.1 (www.appliedbiosystems.com). *V. vinifera* cv. Cabernet Sauvignon berry samples were collected from a commercial vineyard near Osoyoos, B.C., and immediately snap frozen. Exocarp, mesocarp (berry 'flesh' tissue), seed, root, leaf, and flower tissue originated from vines collected during the 2003 season. Tendril and stem tissues were collected from vines grown in a greenhouse at UBC Vancouver. Primers for real time RT-PCR are given in Table S2. Dissociation curve analyses and sequencing of products were used to confirm gene specificity for each of the amplicons (data not shown). Flower was used as the calibrator sample because this was the tissue with the lowest differences in ΔCt values among the different genes tested. Efficiencies of all primer pairs were above 1.8, and data were corrected accordingly.

4.2. Cloning and functional expression of FAOMT

Genbank accession number EC932040 is an EST derived from a cDNA clone from *V. vinifera* cv. Cabernet Sauvignon (Peng et al., 2007). The respective cDNA clone was sequenced in both directions using M13F and M13R primers and completely overlapping bidirectional sequence reads were obtained. The full length cDNA was cloned in-frame with an N-terminal 6x His tag using NdeI and HindIII restriction enzyme sites of the pET28b + cloning vector (Novagen, www.emdbiosciences.com) by the sticky end PCR method (Zeng, 1998). Polymerase chain reaction using the primers given in Table S2 was carried out with Platinum Pfx DNA polymerase (www.invitrogen.com) in a Robocycler® 96 gradient cycler (Stratagene, La Jolla, CA, USA) with the following parameters: 94 °C for 4 min, followed by 40 cycles at 94 °C for 30 s, 55 °C for 30 s, 68 °C for 1 min. After transformation to *E. coli* TOP10 competent cells (www.invitrogen.com) for sequencing purposes, the correct plasmid was subsequently transformed to BL21DE3 protein expression competent cells (Novagen). The pET28b + empty vector was used as a control. After initial growth at 37 °C, IPTG-induced cultures were transferred to 20 °C and 200 rpm overnight for protein expression. Bacterial pellets were washed twice using His-trap column binding buffer (20 mM $NaPO_4$, 500 mM NaCl, 30 mM imidazole, pH 7.4, 10% glycerol, Complete® EDTA-free proteinase inhibitor (Roche, www.roche.com)). His tag expressed protein was purified using His spin trap columns eluting the protein in two separate fractions according to the manufacturers' protocol (GE Healthcare, www.gehealthcare.com). The eluted proteins in 20 mM $NaPO_4$, 500 mM NaCl, 500 mM imidazole, pH 7.4 and 10% glycerol were buffer exchanged and further purified using an Amicon Ultra 10 kDa cutoff filter (Millipore, http://www.Millipore.com). The buffer was exchanged to 10% glycerol, 50 mM Bis–Tris propane, pH 8.5, and then the protein was aliquoted and stored at −80 °C. The N-terminus contains a 20 amino acid long His-tag, which was not removed because previous studies showed no effect on turnover rate of flavonoids in iceplant PFOMT experiments (Kopycki et al., 2008; Zubieta et al., 2001). Protein concentration was determined at OD_{280} using the calculated extinction coefficient for His-tagged FAOMT.

4.3. Enzyme purity analysis

Precast NuPAGE Novex® Bis–Tris 4–12% gels were run in 1X MES buffer on the NuPAGE gel electrophoresis system under reducing conditions and stained with Simply Blue Safe Stain (Invitrogen). As a size marker, 5 µl Mark 12 protein ladder was used (Invitrogen). Various enzyme purification stages indicated that the His-tagged FAOMT was purified nearly to homogeneity, with a molecular weight of approximately 29 kDa (Fig. S2A).

The isolated His tag protein was also analyzed for purity using matrix-assisted laser desorption ionization time-of-flight (MALDI-TOF) on a Voyager-DE STR 4311 system (Applied Biosystems, www.appliedbiosystems.com) (Fig. S2B). After desalting for 3 h using drop dialysis with a 0.025 µm pore 25 mm nitrocellulose disk (Millipore), the protein was mixed in equal amounts with sinapinic acid. Settings used were linear mode of operation, positive polarity, 25,000 V accelerating voltage, 93% grid voltage,

0.15% guide wire, and 1000 nsec extraction delay time. Mass acquisition range was 2000–100,000 Da. 100 laser shots were carried out to acquire the spectrum with a laser intensity of 2431 at 20 Hz.

4.4. Enzyme assays using the heterologous FAOMT

Most anthocyanin, anthocyanidin, and flavonoid substrates were purchased from Extrasynthese (www.extrasynthese.com); petunidin 3-*O*-glucoside (**22**) was from Apin Chemicals (www.apinchemicals.com), CoA esters (**32**) were from TransMIT Flavonoidforschung (www.transmit.de), and keracyanin (cyanidin 3-*O*-rutinoside, **26**), SAM, caffeic acid (**30**), myricetin (**9**), quercetin (**6**), isorhamnetin, (+)-catechin (**28**), and (−)-epi-catechin (**29**) were from Sigma–Aldrich (www.sigmaaldrich.com). Substrates were weighed in volumetric flasks and dissolved using sonication in MeOH-5 mM HCl (1:9). Flavonoid glucosides and dihydroquercetin (**7**) were dissolved in MeOH-5 mM HCl (1:1). Quercetin (**6**) was dissolved in DMSO, and subsequently diluted to MeOH-DMSO (1:1). Myricetin (**9**) was dissolved in MeOH-5 mM HCl (7:3). Caffeic acid (**30**), 4-hydroxybenzoate (**31**), CoA esters (**32**) and the catechins (**28, 29**) were dissolved in H_2O. Glycosylated substrates were aliquoted and stored at −80 °C in the dark for up to two months.

Enzyme assays were performed in MOPSO, Citrate, MES, or Bis–Tris propane buffers (Sigma–Aldrich) in their respective pH ranges, using 33.6 ng His-tag purified protein. The pH for the enzyme analyses ranged from pH 2.9 through pH 9.4, with pH 0.2 intervals between pH 7.6 and pH 9.1. Substrate concentrations used were between 0.1 μM and 150 μM. Optimal assays were performed at pH 8.5 in 50 mM Bis–Tris propane buffer at 49 °C, as tested using quercetin 3-*O*-glucoside (**10**) and cyanidin 3-*O*-glucoside (**18**). HCO_2H was used to adjust the pH (Fluka, www.sigmaaldrich.com). Prior to the assays, a freshly thawed enzyme aliquot was diluted to an appropriate concentration in 10% glycerol containing BTP buffer at pH 8.5 on ice. As controls, either His-tag purified and buffer exchanged pET28 empty vector for residual bacterial protein activity, or boiled FAOMT enzyme was used. Temperature optima were tested between 0 and 65 °C, with 2 degree intervals between 40 and 55 °C, using 84 ng purified protein per assay. Optimum $MgCl_2$ (Sigma–Aldrich) concentration was tested using 0–10 mM $MgCl_2$. Optimum SAM concentration was determined between 0 and 1000 μM SAM. Assays were checked for linearity between 0 and 60 min and determined to be linear between 5 and 45 min. Temperature stability of substrates was tested under assay conditions but using eight different temperatures in between 0 °C and 55 °C. Assays were performed in triplicate for either 18 or 36 min using all substrates combined, each at a concentration of 5 μM.

For substrate specificity, assays were performed under linear conditions with 8.75 ng purified protein, using 4 μM of each substrate and 10 min incubation at 35 °C. These assays were performed in a total volume of 100 μl using 50 mM Bis–Tris propane pH 8.5, 0.1 mg ml^{-1} BSA, 7 mM $MgCl_2$, 500 μM SAM. The substrate conversion rate was determined by the amount of substrate lost after incubation with the enzyme as long as a methylated product could be determined for each substrate (Yoon et al., 2005). Control assays with boiled enzymes were carried out simultaneously. Substrates that did not show any conversion of substrate were also tested with enzyme concentrations of up to 500 ng protein. The reactions were transferred to ice and stopped by addition of $CHCl_3$:MeOH–HCl (2% v/v) (400 μl, 2:1), followed by immediate vortexing for 10 s and subsequent centrifugation at 15,800*g* for 2 min, resulting in a Folch separation (Folch et al., 1957). The upper phase (~200 μl) was collected and transferred to a 2 ml opaque glass vial with glass insert. LC–MS analysis was performed on an LC/MSD Trap XCT Plus with an Agilent 1100 Series front-equipped with a diode array detector (DAD) (Agilent Technologies, www.home.agilent.com) at a rate of 0.85 ml min^{-1} at 350 bar over a Zorbax SB-C18 column (4.6 × 150 mm, 3.5 μM) heated at 70 °C (Agilent Technologies). HCO_2H at 0.2% was used as solvent A, and 0.2% HCO_2H in CH_3CN (EMD Chemicals) as solvent B, with the following gradient: 5% solvent B to 14% solvent B after 7 min, then increased to 60% solvent B after 15 min, and kept at 60% solvent B for another 5 min. After each sample run, the column was set to calibrate for 5 min at 5% solvent B. The LC was connected to an MS ESI set at 350 °C, positive ion scanning mode, nebulizer set at 60 psi, 12 l min^{-1} N2 gas flow, ion trap scanning between 40 *m*/*z* to 700 *m*/*z*. The DAD recorded spectra from 190 to 600 nm. Anthocyanins and anthocyanidins were analyzed at 520 nm with a bandwidth of 10 nm. Flavonoid glucosides and aglycones were analyzed at 365 nm with a bandwidth of 16 nm. CoAs were separated and identified as described using Nucleodur C18ec 250/4 (Macherey & Nagel, Germany) (Ibdah et al., 2003).

For the determination of enzyme kinetics, assays were performed under linear and optimized conditions (49 °C, pH 8.5) with less than 10% substrate conversion for all substrates using 0.7 ng protein per each 100 μl assay for quercetin 3-*O*-glucoside (**10**) or using 0.875 ng per assay for cyanidin 3-*O*-glucoside (**18**) in freshly prepared solutions. All assays were performed in triplicate with at least 10 different substrate concentrations per K_m experiment, ranging up to 10 times the calculated K_m. Calculations of product formation were based on standard curves for the respective products, which were determined via assays under identical conditions as used for the substrates. Peak areas of the optimal DAD spectra were integrated manually and converted to product concentrations based on the standard curves. The spreadsheet, Anemona.xlt, was used for determining Michaelis–Menten kinetics using non-linear regression for calculation of the curves (Hernandez and Ruiz, 1998).

4.5. Protein alignments and phylogenetic analysis

In order to find orthologs that are closely related to *faomt* in plant species that are well known for accumulation of anthocyanins or other flavonoids, the non-human non-mouse EST database (est_others) at NCBI was searched using tblastn. Two full length *omt* sequences were assembled from apple and snapdragon ESTs showing high similarity to *faomt* (Dong et al., 1998; Martin et al., 1991).

To determine sequence identity percentages between Type 2 methyltransferases, the program DNASTAR MegAlign was used, incorporating the BLOSUM series protein weight matrix with ClustalW alignment and settings of gap penalty at 10 and gap length penalty at 0.2. Prediction of the secondary structure of the protein was performed using APSSP2 by online submission of the full length protein (http://www.imtech.res.in/raghava/apssp2/). The output displays coil, helix, or strand prediction for each amino acid and a probability score of 0.5–1.0 (Raghava, 2002). In the alignment only the probabilities of helix (alpha helix) or strand (beta sheet) of 0.6 and higher are indicated.

Representative Types 1 and 2 methyltransferase proteins were aligned using an anchored dialign online submission with Threshold = 2 as the setting (http://dialign.gobics.de/anchor/submission.php). The alignment was hand corrected in Genedoc. The aligned sequences were subsequently submitted to Phyml online (http://www.atgc-montpellier.fr/phyml/) which searches for the best tree among five random trees using SPRs and the LG model of amino acid substitution (Hordijk and Gascuel, 2005; Le and Gascuel, 2008). The best BioNJ tree was automatically selected. The proportion of invariant sites was estimated to be 0.022, the substitution rate number was set at 4, and the gamma distribution pattern was estimated to be 1.9448. For subsequent maximum likelihood bootstrapping analyses, the initial results for

the proportion of invariable sites and gamma distribution were set and bootstrapping was done for 500 repetitions (Guindon and Gascuel, 2003). The results of the bootstrapping were converted to percentages and bootstrap values lower than 50% were removed.

Acknowledgements

We thank Tatiana Pirogovskaia and Merinda Deng for carrying out the RNA isolations. We also thank Lina Madilao for help in developing the LC–MS methods and Suzanne Perry for the MALDI-TOF analysis. We gratefully acknowledge funding for this research from Genome Canada and Genome British Columbia, as well as additional funding for this work from a Natural Sciences and Engineering Research Council of Canada (NSERC) Discovery Grant award to STL. We thank the Province of British Columbia and the BC wine industry for their continued support of research activities in the University of British Columbia Wine Research Centre. Materials described here can be provided upon request.

Appendix A. Supplementary material

Supplementary data associated with this article can be found, in the online version, at doi:10.1016/j.phytochem.2010.05.027.

References

Ageorges, A., Fernandez, L., Vialet, S., Merdinoglu, D., Terrier, N., Romieu, C., 2006. Four specific isogenes of the anthocyanin metabolic pathway are systematically co-expressed with the red colour of grape berries. Plant Sci. 170, 372–383.

Bailly, C., Cormier, F., Bao Do, C., 1997. Characterization and activities of S-adenosyl-l-methionine: cyanidin 3-glucoside 3′-*O*-methyltransferase in relation to anthocyanin accumulation in *Vitis vinifera* cell suspension cultures. Plant Sci. 122, 81–89.

Boss, P.K., Davies, C., Robinson, S.P., 1996a. Analysis of the expression of anthocyanin pathway genes in developing *Vitis vinifera* L. Cv Shiraz grape berries and the implications for pathway regulation. Plant Physiol. 111, 1059–1066.

Boss, P.K., Davies, C., Robinson, S.P., 1996b. Anthocyanin composition and anthocyanin pathway gene expression in grapevine sports differing in berry skin colour. Aust. J. Grape Wine Res. 2, 163–170.

Boulton, R., 2001. The copigmentation of anthocyanins and its role in the color of red wine: a critical review. Am. J. Enol. Vitic. 52, 67–87.

Busam, G., Junghanns, K.T., Kneusel, R.E., Kassemeyer, H.H., Matern, U., 1997. Characterization and expression of caffeoyl-coenzyme A 3-*O*-methyltransferase proposed for the induced resistance response of *Vitis vinifera* L. Plant Physiol. 115, 1039–1048.

Cacace, S., Schroder, G., Wehinger, E., Strack, D., Schmidt, J., Schroder, J., 2003. A flavonol *O*-methyltransferase from *Catharanthus roseus* performing two sequential methylations. Phytochemistry 62, 127–137.

Castellarin, S., Di Gaspero, G., 2007. Transcriptional control of anthocyanin biosynthetic genes in extreme phenotypes for berry pigmentation of naturally occurring grapevines. BMC Plant Biol. 7:46.

Castellarin, S., Di Gaspero, G., Marconi, R., Nonis, A., Peterlunger, E., Paillard, S., Adam-Blondon, A.-F., Testolin, R., 2006. Colour variation in red grapevines (*Vitis vinifera* L.): genomic organisation, expression of flavonoid 3′-hydroxylase, flavonoid 3′,5′-hydroxylase genes and related metabolite profiling of red cyanidin-/blue delphinidin-based anthocyanins in berry skin. BMC Genomics 7:12.

D'Auria, J.C., Chen, F., Pichersky, E., 2003. The SABATH family of methyltransferases in *Arabidopsis thaliana* and other plant species. In: Romeo, J.T. (Ed.), Recent Advances in Phytochemistry, vol. 37. Elsevier Science Ltd., Oxford, pp. 253–283.

de Pascual-Teresa, S., Sanchez-Ballesta, M., 2008. Anthocyanins: from plant to health. Phytochem. Rev. 7, 281–299.

Do, C.B., Cormier, F., Nicolas, Y., 1995. Isolation and characterization of a UDP-glucose: cyanidin 3-*O*-glucosyltransferase from grape cell suspension cultures (*Vitis vinifera* L.). Plant Sci. 112, 43–51.

Dong, Y.H., Beuning, L., Davies, K., Mitra, D., Morris, B., Kootstra, A., 1998. Expression of pigmentation genes and photo-regulation of anthocyanin biosynthesis in developing Royal Gala apple flowers. Aust. J. Plant Physiol. 25, 245–252.

Downey, M.O., Dokoozlian, N.K., Krstic, M.P., 2006. Cultural practice and environmental impacts on the flavonoid composition of grapes and wine: a review of recent research. Am. J. Enol. Vitic. 57, 257–268.

Downey, M.O., Harvey, J.S., Robinson, S.P., 2003. Synthesis of flavonols and expression of flavonol synthase genes in the developing grape berries of Shiraz and Chardonnay (*Vitis vinifera* L.). Aust. J. Grape Wine Res. 9, 110–121.

Felle, H.H., 2005. PH regulation in anoxic plants. Ann. Bot. 96, 519–532.

Ferrer, J.-L., Zubieta, C., Dixon, R.A., Noel, J.P., 2005. Crystal structures of alfalfa caffeoyl coenzyme A 3-*O*-methyltransferase. Plant Physiol. 137, 1009–1017.

Folch, J., Lees, M., Stanley, G.H.S., 1957. A simple method for the isolation and purification of total lipides from animal tissues. J. Biol. Chem. 226, 497–509.

Ford, C.M., Boss, P.K., Hoj, P.B., 1998. Cloning and characterization of *Vitis vinifera* UDP-glucose:flavonoid 3-*O*-glucosyltransferase, a homologue of the enzyme encoded by the maize bronze-1 locus that may primarily serve to glucosylate anthocyanidins in vivo. J. Biol. Chem. 273, 9224–9233.

Forkmann, G., Heller, W., 1999. Biosynthesis of flavonoids. In: Barton, D., Nakanishi, K., Meth-Cohn, O. (Eds.), Comprehensive Natural Products Chemistry, vol. 2. Elsevier, Oxford, pp. 713–748.

Garcia-Alonso, M., Minihane, A.-M., Rimbach, G., Rivas-Gonzalo, J.C., de Pascual-Teresa, S., 2009. Red wine anthocyanins are rapidly absorbed in humans and affect monocyte chemoattractant protein 1 levels and antioxidant capacity of plasma. J. Nutr. Biochem. 20, 521–529.

Guindon, S., Gascuel, O., 2003. A simple, fast, and accurate algorithm to estimate large phylogenies by maximum likelihood. Syst. Biol. 52, 696–704.

Hernandez, A., Ruiz, M.T., 1998. An EXCEL template for calculation of enzyme kinetic parameters by non-linear regression. Bioinformatics 14, 227–228.

Hordijk, W., Gascuel, O., 2005. Improving the efficiency of SPR moves in phylogenetic tree search methods based on maximum likelihood. Bioinformatics 21, 4338–4347.

Hrazdina, G., Jensen, R.A., 1992. Spatial organization of enzymes in plant metabolic pathways. Ann. Rev. Plant Phys. 43, 241–267.

Ibdah, M., Zhang, X.-H., Schmidt, J., Vogt, T., 2003. A Novel Mg^{2+}-dependent *O*-methyltransferase in the phenylpropanoid metabolism of *Mesembryanthemum crystallinum*. J. Biol. Chem. 278, 43961–43972.

Jackman, R.L., Smith, J.L., 1996. Anthocyanins and betalains. In: Hendry, G.A.F., Houghton, J.D. (Eds.), Natural Food Colorants. Chapman and Hall, London, pp. 244–309.

Kopycki, J.G., Rauh, D., Chumanevich, A.A., Neumann, P., Vogt, T., Stubbs, M.T., 2008. Biochemical and structural analysis of substrate promiscuity in plant Mg^{2+}-dependent *O*-methyltransferases. J. Mol. Biol. 378, 154–164.

Le, S.Q., Gascuel, O., 2008. An improved general amino acid replacement matrix. Mol. Biol. Evol. 25, 1307–1320.

Lila, M.A., 2004. Anthocyanins and human health: an in vitro investigative approach. J. Biomed. Biotechnol. 5, 306–313.

Lücker, J., Laszczak, M., Smith, D., Lund, S.T., 2009. Computational approach to the generation of an improved predicted peptide database from EST data and application to iTRAQ analyses in grape (*Vitis vinifera* cv. Cabernet Sauvignon) berries at ripening initiation. BMC Genomics 10:50.

Lukacin, R., Matern, U., Specker, S., Vogt, T., 2004. Cations modulate the substrate specificity of bifunctional class I *O*-methyltransferase from *Ammi majus*. FEBS Lett. 577, 367–370.

Lund, S.T., Peng, F.Y., Nayar, T., Reid, K.E., Schlosser, J., 2008. Gene expression analyses in individual grape (*Vitis vinifera* L.) berries during ripening initiation reveal that pigmentation intensity is a valid indicator of developmental staging within the cluster. Plant Mol. Biol. 68, 301–315.

Martin, C., Prescott, A., Mackay, S., Bartlett, J., Vrijlandt, E., 1991. Control of anthocyanin biosynthesis in flowers of *Antirrhinum majus*. Plant J. 1, 37–49.

Mori, K., Goto-Yamamoto, N., Kitayama, M., Hashizume, K., 2007. Loss of anthocyanins in red-wine grape under high temperature. J. Exp. Bot. 58, 1935–1945.

Noel, J.P., Dixon, R.A., Pichersky, E., Zubieta, C., Ferrer, J.L., 2003. Structural, functional, and evolutionary basis for methylation of plant small molecules. In: Romeo, J.T. (Ed.), Recent Advances in Phytochemistry, vol. 37. Elsevier Science, Oxford, pp. 37–58.

Peng, F.Y., Reid, K.E., Liao, N., Schlosser, J., Lijavetzky, D., Holt, R., Martínez Zapater, J.M., Jones, S., Marra, M., Bohlmann, J., Lund, S.T., 2007. Generation of ESTs in *Vitis vinifera* wine grape (Cabernet Sauvignon) and table grape (Muscat Hamburg) and discovery of new candidate genes with potential roles in berry development. Gene 402, 40–50.

Poustka, F., Irani, N.G., Feller, A., Lu, Y., Pourcel, L., Frame, K., Grotewold, E., 2007. A trafficking pathway for anthocyanins overlaps with the endoplasmic reticulum-to-vacuole protein-sorting route in Arabidopsis and contributes to the formation of vacuolar inclusions. Plant Physiol. 145, 1323–1335.

Raghava, G.P.S., 2002. A combination method for protein secondary structure prediction based on neural network and example based learning. CASP V, A-132.

Reid, K., Olsson, N., Schlosser, J., Peng, F., Lund, S., 2006. An optimized grapevine RNA isolation procedure and statistical determination of reference genes for real-time RT-PCR during berry development. BMC Plant Biol. 6:27.

Schaefer, H.M., McGraw, K., Catoni, C., 2008. Birds use fruit colour as honest signal of dietary antioxidant rewards. Funct. Ecol. 22, 303.

Shao, L., Shu, Z., Sun, S.-L., Peng, C.-L., Wang, X.-J., Lin, Z.-F., 2007. Antioxidation of anthocyanins in photosynthesis under high temperature stress. J. Integr. Plant Biol. 49, 1341–1351.

Spayd, S.E., Tarara, J.M., Mee, D.L., Ferguson, J.C., 2002. Separation of sunlight and temperature effects on the composition of *Vitis vinifera* cv. Merlot berries. Am. J. Enol. Vitic. 53, 171–182.

Sroka, Z., 2005. Antioxidative and antiradical properties of plant phenolics. Z. Naturforsch. (C) 60, 833–843.

The French–Italian Consortium for Grapevine Genome Characterization, 2007. The grapevine genome sequence suggests ancestral hexaploidization in major angiosperm phyla. Nature 449, 463–467.

Vogt, T., 2004. Regiospecificity and kinetic properties of a plant natural product *O*-methyltransferase are determined by its N-terminal domain. FEBS Lett. 561, 159–162.

Wang, H., Race, E.J., Shrikhande, A.J., 2003. Anthocyanin transformation in Cabernet Sauvignon wine during aging. J. Agric. Food Chem. 51, 7989–7994.

Watson, B., 2003. Evaluation of wine grape maturity. In: Hellman, E.W. (Ed.), Oregon Viticulture. Oregon State University Press, Corvallis, OR, pp. 235–245.

Winkel-Shirley, B., 1999. Evidence for enzyme complexes in the phenylpropanoid and flavonoid pathways. Physiol. Plantarum 107, 142–149.

Yoon, Y., Yi, Y.S., Lee, Y., Kim, S., Kim, B.G., Ahn, J.-H., Lim, Y., 2005. Characterization of *O*-methyltransferase ScOMT1 cloned from *Streptomyces coelicolor* A3(2). Biochim. Biophys. Acta 1730, 85–95.

Zeng, G., 1998. Sticky-end PCR: new method for subcloning. Biotechniques 25, 206–208.

Zubieta, C., He, X.-Z., Dixon, R.A., Noel, J.P., 2001. Structures of two natural product methyltransferases reveal the basis for substrate specificity in plant *O*-methyltransferases. Nat. Struct. Biol. 8, 271–279.